Supramolecular Fluids Hot Paper

How to cite: *Angew. Chem. Int. Ed.* **2021**, *60*, 7540–7546
International Edition: doi.org/10.1002/anie.202015800
German Edition: doi.org/10.1002/ange.202015800

A New Type of Supramolecular Fluid Based on H_2O–Alkylammonium/Phosphonium Solutions

Carlos López-Bueno, Carlos Herreros-Lucas, Manuel Suárez-Rodríguez, Marius R. Bittermann, Alfredo Amigo, Sander Woutersen, María Giménez-López, and Francisco Rivadulla**

Abstract: *Here we show that by adjusting the concentration of tetrabutyl ammonium and phosphonium salts in water (≈1.5–2.0 m), hydrophobic solvation triggers the formation of a unique, highly incompressible supramolecular liquid, with a dynamic structure similar to clathrates, involving essentially all H_2O molecules of the solvent. Despite the increasing local order, the thermal diffusivity, and compressibility of these supramolecular liquids is strongly decreased with respect to bulk water due to slower relaxation dynamics. The results presented in this paper open an avenue to design a new family of supramolecular fluids, stable under atmospheric conditions, which can find important technological applications in energy storage and conversion.*

Dissolving small non (or moderate)-polar molecules in water induces the formation of local ice-like structures around them.[1–4] Above a certain concentration of the solute, and under conditions of high pressure and low temperature, these host-guest hydrates can form crystalline solids, so-called clathrate hydrates, a vast class of materials with important applications in gas separation, storage and transportation.[5–7] When the host molecule takes part within the multi-polyhedral structure of hydrogen-bonded water, semi-clathrate hydrates are formed. This is the case for tetrabutyl ammonium bromide (TtBABr) and other quaternary ammonium salts, in which the anions incorporate into the hydrogen-bonded water networks which enclose $TtBA^+$ cations.[8] Interestingly, once crystallized several semi-clathrates of composition $TtBABr{\cdot}x\,H_2O$ with $x \approx 17$–32 are stable under ambient pressure, and melt above 9–12 °C.[7,9–11] Nevertheless, most of the investigations to date were limited to the study of the crystalline phase, overlooking the structure of the molten (liquid) phase. Strong evidence supporting the existence of rigid structures of H_2O molecules around hydrophobic groups in the liquid phase has accumulated over the years.[2,3] However, these are considered to affect a limited number of water molecules; thus water is assumed to retain most of its thermodynamic bulk properties, except for those in crowded environments.[12] Here we demonstrate evidence for the formation of a stable supramolecular liquid with a composition $\approx TtBABr{\cdot}32\,H_2O$, at a relatively low concentration of TtBABr ≈ 1.8 m (≈3 mol %). The structure of $TtBA^+$ ions induces the formation of large hydration spheres, involving all molecules of the solvent. This fluid is shown to be highly incompressible and presents an important reduction of its thermal diffusivity and heat capacity with respect to bulk water, despite its increasing molecular order. We report also similar characteristics in tetrabutyl-ammonium chloride and tetrabutyl-phosphonium bromide, suggesting that other polyalkyl pnictogen salts could show this type of supramolecular liquid behavior. Given the nature of these complex fluids, unforeseen applications in energy related areas as well as sequestering agents of small nonpolar molecules could be inferred.

We prepared a series of solutions with different concentrations of TtBABr, from 0.2 m to 18 m. Calorimetric studies (DSC, see Figure 1) show that the behavior up to ≈0.6 m is similar to that of pure water, with an exothermic peak at the temperature of formation of ice and an endothermic peak at the melting temperature at 0 °C. At [TtBABr] ≥ 0.6 m, the peaks of ice-melting decrease progressively until practically disappearing at ≈1.8 m and beyond. At this concentration, exothermic/endothermic peaks characteristic of the formation/melting of the crystalline clathrate hydrate lattice show up. A comparison of the temperatures of formation (265 K) and melting (282 K, 286 K), and the enthalpy of fusion $\Delta H_{fus} = 202\ J\,g^{-1}$, with values in the literature,[11,13–15] shows that the clathrate formed from cooling the 1.8 m solution is $TtBABr{\cdot}32H_2O$.

This is almost exactly the $TtBABr{:}H_2O$ molecular ratio in a solution of 1.8 m. The DSC scan for the 3.5 m solution ($TtBABr{:}H_2O$ molar ratio $x \approx 17$) shows a double peak structure at $T_m \approx 282$–285 K, similar to the report by Rodionova et al.[11] for $TtBABr{\cdot}x\,H_2O$, $x \approx 24$, and the complete suppression of the ice-melting peak. By comparing the area of

[*] C. López-Bueno, Dr. C. Herreros-Lucas, M. Suárez-Rodríguez, Prof. M. Giménez-López, Prof. F. Rivadulla
CIQUS, Centro de Investigación en Química Biolóxica e Materiais Moleculares, Universidade de Santiago de Compostela
15782-Santiago de Compostela (Spain)
E-mail: maria.gimenez.lopez@usc.es
f.rivadulla@usc.es

M. R. Bittermann, Prof. S. Woutersen
Institute of Physics (MB) and Van't Hoff Institute for Molecular Sciences (SW), University of Amsterdam
Science Park 904, 1098 XH Amsterdam (The Netherlands)

Prof. A. Amigo
Departamento de Física Aplicada, Facultad de Física, Universidade de Santiago de Compostela
15782-Santiago de Compostela (Spain)

Supporting information and the ORCID identification number(s) for the author(s) of this article can be found under: https://doi.org/10.1002/anie.202015800.

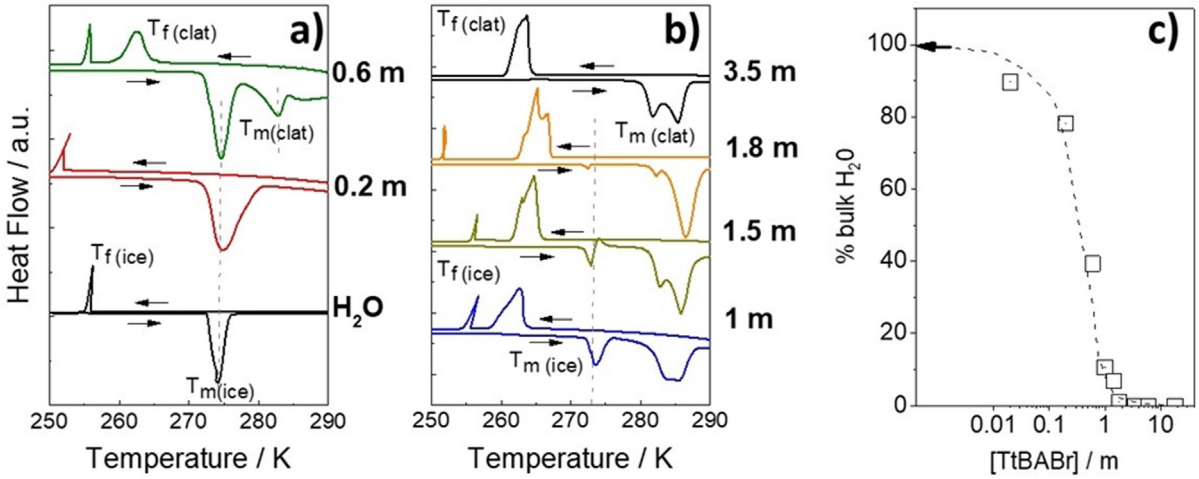

Figure 1. a) and b) DSC scans of pure water and other six solutions with an increasing concentration of TtBABr. The exo/endothermic peaks at T_f(ice)/T_m(ice), corresponding to the formation/melting of ice, are barely visible at concentrations above 1.8 m. Instead, only the peaks at T_f(clat) and T_m(clat), signaling the formation and melting of the crystalline clathrate hydrates, are observed. The double-peak shape of T_m(clat) between 1–3.5 m is characteristic of TtBABr·x H_2O x = 17–32.[11] The large endothermic peak at T_f(ice) was cut to fit in the same scale. c) Fraction of ice-forming bulk water extracted from the comparison of the areas of the melting peaks at 273 K of different solutions and pure water. The data show that above ≈1.8 m most of the water molecules are forming the crystalline lattice of the clathrate structure at low temperature. The arrow marks the value for pure water. The dashed line is a guide to the eye.

the endothermic peaks at 0 °C with that of pure water, we extracted the fraction of free water (available to form ice) for each solution. At 1.8 m, less than 1% of the solvent water molecules are available to form ice, while no free water is detected in the 3.5 m solution. Thus, the calorimetric experiments confirm the formation of crystalline clathrate hydrates at low temperature, which around ≈1.8–3.5 m decompose into a liquid state of the same composition, that is, all water molecules of the solvent participate in the formation of the solid clathrate hydrate at low temperature.

To analyze the structure of the liquid phase at these concentrations, the average structural arrangement of water molecules and their orientational motion was probed by adiabatic compressibility, thermal diffusivity, and conventional temperature dependence IR absorption of the O-H stretching mode. The experiments for different concentrations of TtBABr are discussed below.

Thermal contraction makes most liquids less compressible as temperature decreases. However, water shows a minimum compressibility, K, at T_{min} ≈ 330 K, with a rapid increase below this temperature due to the formation of a complex H-bonding network (Figure 2a).[16,17] As the energy to be minimized in water is H-bonding, the temperature dependence of K is dominated by thermal fluctuations above $K(T_{min})$, and by structural fluctuations below $K(T_{min})$.[18] H-bonds can also store a substantial amount of energy, resulting in a C_p minimum at ≈330 K (Figure 2b). Consequently, any extensive modification of the H-bond network of bulk liquid water by hydrophobic solvation should be reflected in the magnitude and temperature dependence of K and C_p.

The results in Figure 2 show that dissolving TtBABr indeed produces a rapid decrease of K and C_p, and the suppression of the minimum in the temperature dependence of both magnitudes. In particular, the decrease of K at low temperatures suggests that the structural fluctuations that

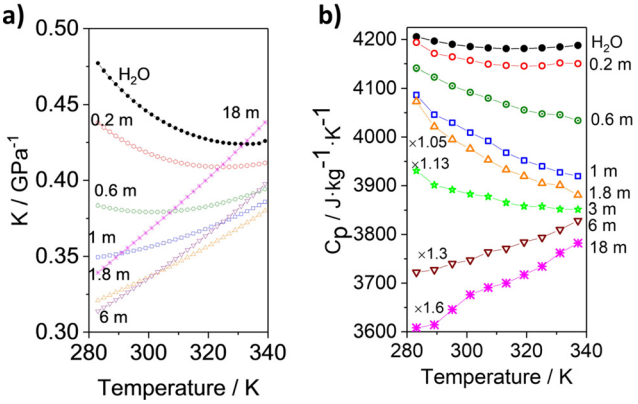

Figure 2. Temperature dependence of the adiabatic compressibility, K (a), and heat capacity, C_p (b), for different concentrations of TtBABr. The curves of $C_p(T)$ were multiplied by a factor (shown) to fit in the same scale.

dominate $K(T < T_{min})$ in bulk water are progressively replaced by thermal fluctuations, as [TtBABr] increases.

C_p also decreases as [TtBABr] increases, reflecting the suppression of the H-bond contribution to energy storage at low temperature. However, the negative dC_p/dT coefficient up to ≈3 m demonstrates that translational and rotational modes (the main contributors to C_p above room temperature in liquid water) are largely suppressed at these concentrations of TtBABr (at least up to 340 K). On the other hand, K increases again at larger [TtBABr], and the characteristic $dK/dT > 0$ and $dC_p/dT > 0$ of molecular liquids is recovered.[17,19–21] Thus, both K(293 K) and dC_p/dT(293 K) show a minimum at [TtBABr] ≈ 1.4–2.2 m (Figure 3 and Figure S1), the concentrations coincident with the hydration numbers of the most stable solid semi-clathrates, TtBABr·x H_2O x = 17–32.[10,11]

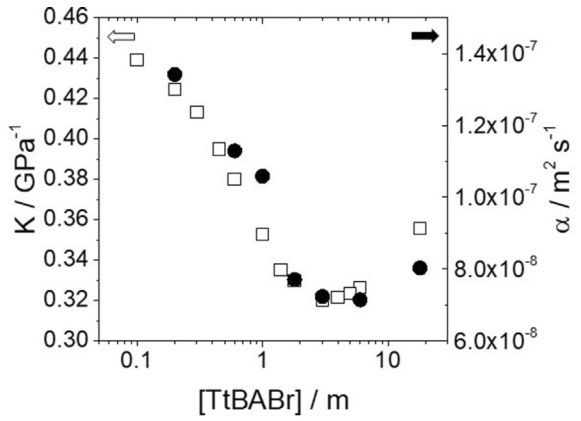

Figure 3. Variation of the room temperature adiabatic compressibility, K (open squares), and thermal diffusivity, α, (closed circles) for different concentrations of TtBABr. The open/solid arrows indicate the values of K/α at 293 K.

The thermal diffusivity, $\alpha = \kappa/(\rho C_p)$ also shows a minimum in the same region as K. The extent and strength of H-bonding is determinant in the energy transfer in liquid water, through coupling of low frequency excitations over various H_2O molecules (see also the thermal conductivity in Figure S1 of the supporting information).[22] The reduction of α is much higher than expected based on a purely local coordination (see Figure S2 and its discussion) and further supports a picture in which hydrophobic solvation of $TtBA^+$ modifies the H-bond structure of bulk water, beyond the most immediate molecular environment. A comparison with the compressibility, thermal diffusivity, and specific heat of other tetra-alkyl ammonium bromide salts, confirms the singularity of the tetrabutyl arrangement (see Figure S3 in the supporting information). This is in agreement with previous works which showed that tetrabutyl and tetraisoamylammonium salts form hydrate clathrates, while quaternary ammonium salts with shorter alkyl chains (methyl, propyl) do not.[8]

Cooling down the 1.8 m solution below the temperature of formation of the solid $TtBABr{\cdot}32\,H_2O$ clathrate does not recover a large thermal conductivity, like in crystalline ice for instance (Figure S1 in the supporting information). This suggests either a poor long-range order, with changing orientation between supramolecular assemblies, or rattling of the $TtBA^+$ chains within the water cages[23] (or a combination of both). This situation resembles more a liquid-glass transition than a true crystallization (like in pure ice for instance) where new and stronger long-range bonds are formed from a disordered liquid.[24]

To follow the changes in the intermolecular hydrogen bonding in more detail, we measured the temperature dependence of the IR absorption of several [TtBABr] solutions (Figure 4). The experiments were performed by dissolving the TtBABr in 4.0% D_2O in H_2O (partially deuterated water) to isolate the contribution from OD stretching and prevent intermolecular coupling. This vibrational mode gives a strong absorption in the IR spectrum at $\approx 2500\ cm^{-1}$, which is very sensitive to the distribution of intermolecular hydrogen bond strengths.[25–28] The rapid increase in frequency at ≈ 1.8–3 m, suggests a change in the arrangement of the H-bonds among water molecules at these compositions (Figure S4).

Increasing the concentration of TtBABr to ≥ 0.6 m results in the formation of a clathrate during cooling across T_f(clat) (Figure 1). The OD stretch band shows changes in its approximately Gaussian shape and intensity across T_f(clat) that are similar in the three solutions (Figure S5 in the supporting information), suggesting similar structural changes in the H-bond network across this transition. Further cooling results in formation of ice below T_f(ice), with a discontinuous softening and narrowing of the stretching mode, and a large increase of the absorption intensity below this temperature. The absorption peak shows a characteristic Lorentzian shape (Figure S6), due to homogeneous broadening by thermal fluctuations in ice. All these effects are the consequence of the stronger and narrower frequency distribution of the intermo-

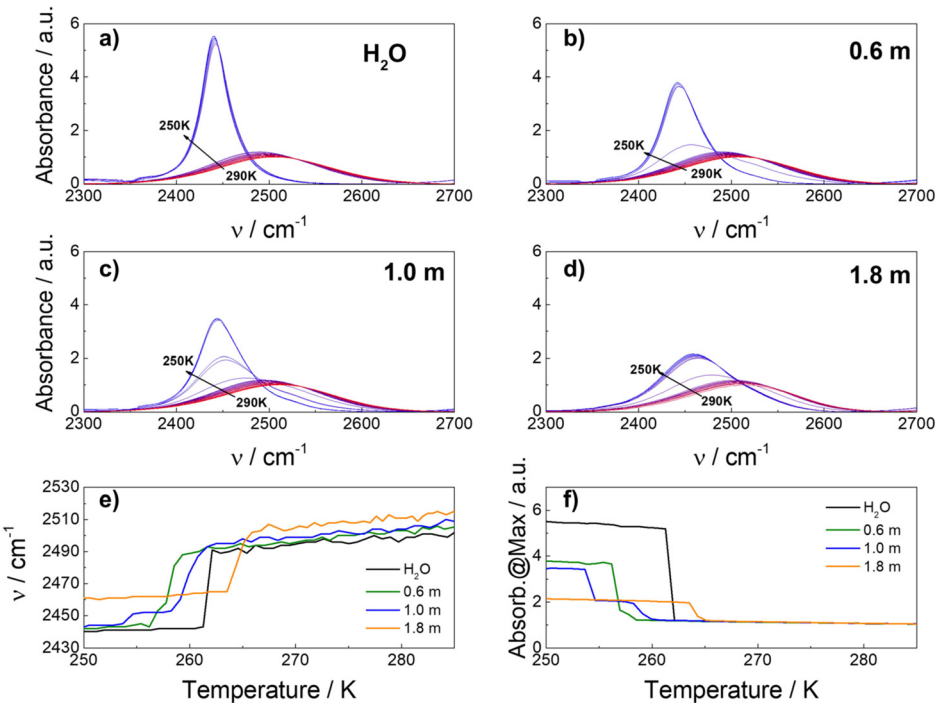

Figure 4. a–d) IR spectra for different concentrations of TtBABr in 4% D_2O in H_2O at different temperatures. The absorbance at $\approx 2500\ cm^{-1}$ corresponds to the stretching mode of the intramolecular OD bonds. All plots in the same scale, for comparison. e) Temperature dependence of the frequency and f) absorption intensity normalized at room temperature.

lecular H-bonds in ice, and the increasing dipole moment with respect to liquid water.[28] The contribution of the ice-peak to the IR spectrum decreases as [TtBABr] increases, due to the decreasing amount of free water.

This can be further appreciated comparing the relative change in the absorbance of the solutions shown in Figure 4 f): The magnitude of the increase at T_f(ice) decreases as the concentration of free water decreases, and disappears completely at 1.8 m. On the other hand, the spectral change at T_f(clat) is the same for the three solutions, suggesting a similar bond rearrangement when the water solutions are cooled across T_f(clat).

The nearly complete absence of spectral changes related to ice formation in the 1.8 m solution seems to confirm that there are no "free" water molecules in this solution, and that the liquid formed upon melting TtBABr·xH$_2$O $x = 17$–32 is a supramolecular liquid, in which individual molecules of TtBABr·xH$_2$O interact loosely amongst each other at room temperature, remaining in a fluid state stable under usual atmospheric conditions.

To further corroborate this interpretation, we show in Figure 5 the ^{79}Br NMR spectra of several solutions with different concentrations of TtBABr, at different temperatures. Br$^-$ ion forms part of the water structure around TtBA in semi-clathrates,[29] which should result in a substantial increase of its rotational time in the liquid phase. Consistent with that, a considerable line-broadening of the ^{79}Br NMR spectra was observed as the concentration of TtBABr approaches 1.8 m (Figure 5 a). The absorption of the 1.8 m solution is completely suppressed at room temperature, and it is progressively recovered above 330–340 K (Figure 5 b). A comparison with a 1.1 m solution of KBr shows that the large broadening and deshielding observed is not compatible with simple bromine hydration or an increase of the viscosity of the solution, as the linewidth broadening is much higher than predicted by Stokes-Einstein equation (see Figure S7 in the supporting information and its discussion). Therefore, it can be concluded that all Br$^-$ ions incorporate to the clathrate structure at 1.8 m; these structures become unstable as temperature increases, and the signal of Br is partially recovered. Additional temperature-dependent ^{79}Br-NMR spectra for different compositions are shown in Figure S8 of the supporting information.

An important aspect of this work is to elucidate whether the interesting properties reported for the liquid phase of ≈1.8 m TtBABr are unique to this system or can be reproduced (or even improved regarding some applications) with other solutes.

We observed that very similar characteristics are obtained with other tetrabutylamonium salts, replacing Br$^-$ by Cl$^-$, for instance (see supporting information Figure S9, and the discussion of the next section). Guided by the intuition of the symmetric disposition of the hydrophobic groups[30] we studied the solutions of tetrabutylphosphonium bromide (TtBPBr).

The DSC scans (Figure S10 in the supporting information) confirm the formation and stability of the hydrate clathrates of the phosphonium salt, with an optimum composition at ≈1.5–3.0 m, like the case of the ammonium salt. The adiabatic compressibility, thermal diffusivity (Figure 6), specific heat, and speed of sound (see also Figure S11 in the supporting information), of the liquid phase show the characteristic anomalies around these concentrations, thus confirming the formation of the supramolecular fluid also with the phosphonium salt.

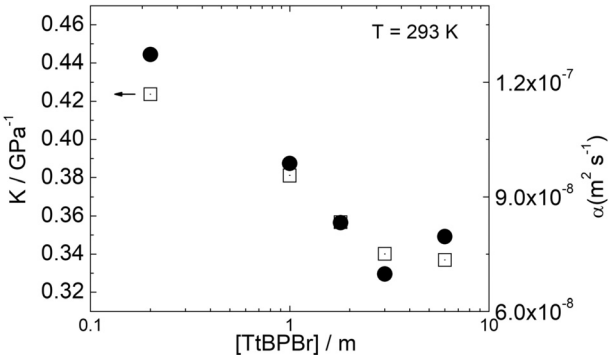

Figure 6. Adiabatic compressibility, K (open squares), and thermal diffusivity, α, (closed circles) for different concentrations of TtBPBr.

Interestingly, these findings point out the possibility of extending the formation of supramolecular liquids to other pnictogen alkyl salts; given the huge number of clathrate-forming molecules,[13] the properties of the supramolecular fluids so designed could be carefully optimized for a particular application.

Next, we describe two electrochemical processes in water, in which the molecular liquids described in this paper could find an application.

The oxidation of Pt^0 in water at positive potentials, that is, Pt + H$_2$O → Pt-OH + H$^+$ + e$^-$ (and its reverse reduction reaction) is a well-known process.[31] To probe whether the supramolecular liquid structure restricts the participation of the water molecules on the redox process occurring on a Pt surface, cyclic voltammogram experiments of Pt nanoparticles (Pt-NPs) on carbon supported on a glassy carbon electrode were performed using TtBABr (1.8 m) water solution as the electrolyte. The voltammogram experiments were compared with that obtained for KBr (1.8 m) water solutions. As shown in Figure 7, Pt-NPs pres-

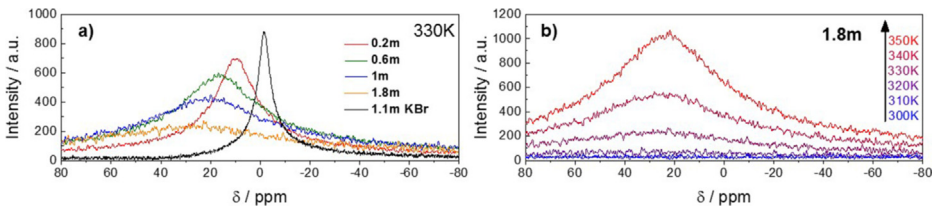

Figure 5. a) ^{79}Br-NMR spectra for solutions with different concentrations of TtBABr at 330 K. The black line centered at $\delta = 0$ corresponds to a 1.1 m solution of KBr (divided by 4 to fit in the same scale) for comparison. b) Temperature dependence of ^{79}Br- NMR absorption for the 1.8 m.

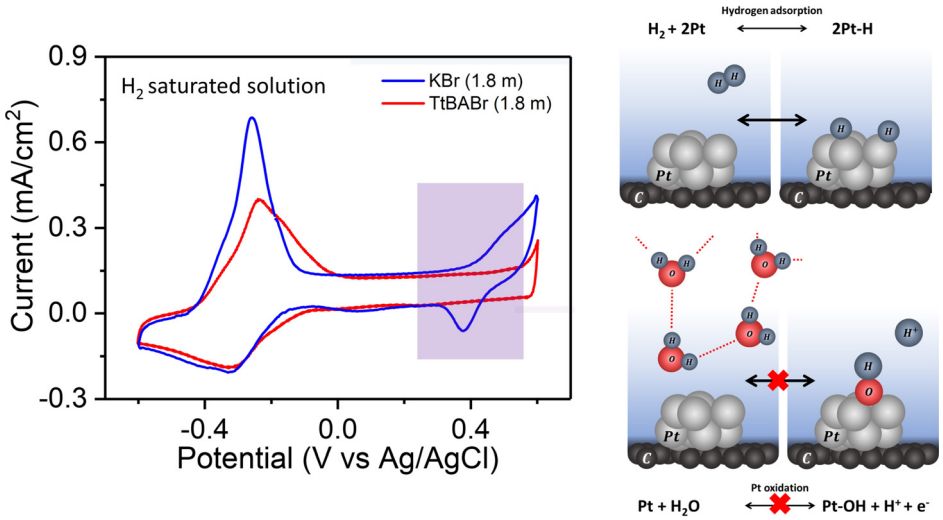

Figure 7. Cyclic voltammograms of Pt/C in hydrogen saturated 1.8 m KBr (blue) and 1.8 m TtBABr (red) solutions at 50 mVs^{-1}. The region between ≈ −0.6 to 0 V corresponds to the adsorption/desorption of hydrogen on the surface of platinum nanoparticles, while that (highlighted) between ≈0.2 to 0.6 V is related to the superficial oxidation/reduction of Pt. The schemes represent these processes; the superficial oxidation/reduction of Pt in water is inhibited in TtBABr 1.8 m due to low reactivity of water molecules when forming liquid clathrates.

ent the expected electrochemically activity in a hydrogen saturated solution of KBr (1.8 m), that is, H_2 molecules show a reversible adsorption/desorption on the Pt surface at negative potentials (from ≈ −0.6 to 0 V), while H_2O molecules oxidize the Pt surface at potential higher than ≈0.4 V.[31] The cathodic peak at ≈0.38 V in the KBr solution corresponds to the reduction of the electrochemically oxidized Pt surface. However, the oxidation of Pt by H_2O is inhibited in the TtBABr (1.8 m) water solution, as reflected in the absence of any measurable faradaic current at positive potentials. It is important to remark that $TtBA^+$ is not blocking the electrode surface, as demonstrated by the fact that Pt is still electrochemically active at negative potentials, where the adsorption/desorption of hydrogen takes place. Therefore, it is the strong interaction among H_2O molecules in the tight structure of the supramolecular liquid what limits their reactivity.

This experiment demonstrates that using TtBABr (1.8 m) as an electrolyte, limits the surface redox reactions on Pt due to the inhibition of the H_2O adsorption, widening the working potential window, which could offer interesting electrochemical applications for these supramolecular liquids.

On the other hand, electrochemical applications of several non-noble metals like Cu are severely limited by their stability on aqueous environment, due to corrosion.[32,33] The electrochemical properties of Cu in the TtBABr supramolecular liquid were investigated in a three-electrode set-up, using Ag/AgCl as the reference electrode and Pt wire the counter electrode. The corrosion of Cu is chemically complex, and apart from the oxidation to copper oxides (Cu_2O), it has been reported an additional two-step process in the presence of Cl^-. In this case, a film of CuCl grows on the surface of the electrode, according to:[34]

$$Cu(s) + Cl^-(aq) \leftrightarrow CuCl(s) + e^- \quad (1)$$

and it then forms a soluble chloro-cuprate (I) species:

$$CuCl(s) + Cl^- \leftrightarrow CuCl_2^-(aq) \quad (2)$$

Figure 8a shows a cyclic voltammogram of a Cu wire in a 1.8 m solution of KCl, showing a redox process around 0 V. The low Coulombic efficiency, that is, the large anodic to cathodic peak current ratio (ia/ic) ≈2.42, confirms that some of the Cu atoms are irreversibly oxidized to $CuCl_2^-$ leaving

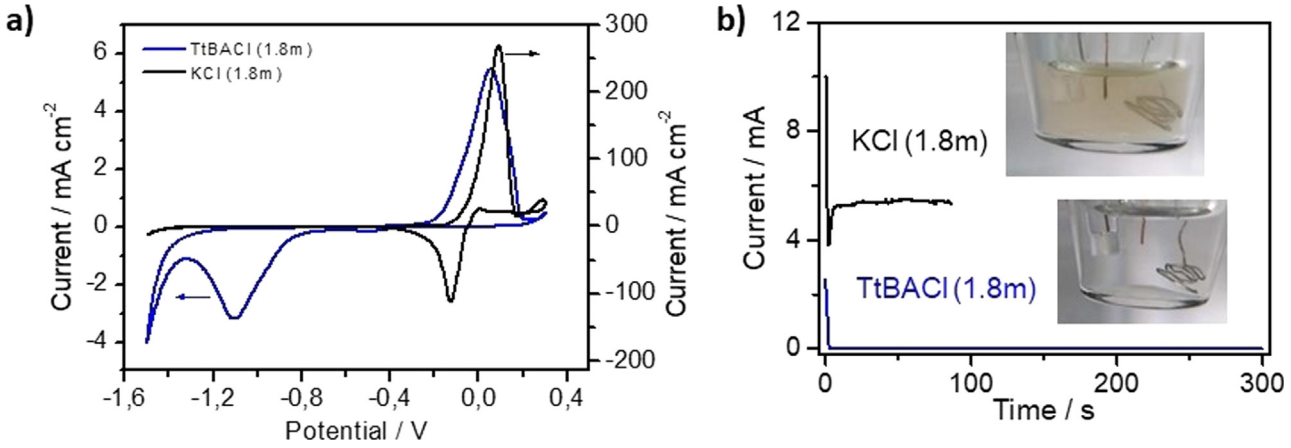

Figure 8. a) Cyclic voltammograms of a Cu wire in 1.8 m KCl (black) and in 1.8 m TtBACl (blue) at 50 mVs^{-1}. b) Chronoamperogram of a Cu wire in 1.8 m KCl (black) and in 1.8 m TtBACl (blue), at 0.3 V.

the electrode surface. Note that current is still positive at potential higher than 0.2 V as the dissolution of Cu leaves fresh Cu atoms which can be further oxidized at positive potentials.

To reduce the reactivity of Cl^- ions in water, we prepared a 1.8 m solution of TtBACl and studied the effect of the formation of a supramolecular clathrate structure on the Cu corrosion. As discussed before, calorimetric DSC experiments (Figure S8) show that the clathrate is formed with the chloride tetrabutylammonium salt, thus retaining Cl^- ions within the hydrate structure.

The corrosion of copper is largely inhibited in the aqueous TtBACl solution; there is a new redox process at ≈ -0.52 V with a small current density and larger potential peak separation $\Delta E = E_a - E_c \approx 1.162$ V (Figure 8a), compared to ≈ 0.216 V in the 1.8 m KCl solution. The oxidized species of Cu appears to be now stabilized towards the reduction, and the formation and loss of $CuCl_2^-$ from the electrode is hindered with respect to that observed in KCl, as the current when decreasing the potential is negative at 0.2 V.

To further demonstrate the stability of Cu in the 1.8 m aqueous solution of TtBACl, chronoamperometry measurements were performed in KCl and TBACl, at a very oxidizing potential of 0.3 V (Figure 8b). The oxidation of Cu in KCl is characterized by a high current density (as expected taking into consideration the current values observed at the same potential in the cyclic voltammogram) and the change of color of the electrochemical solution from transparent to light brown. However, this is not the case for the TtBACl, as shown in the same Figure. Raman spectra (supporting information, Figure S12) confirms the formation of both CuCl and Cu_2O on the surface of the Cu electrode in 1.8 m KCl after chronoamperometry experiments, while only the bands related to the presence of $TtBA^+$ are observed on the Cu electrode used for the experiment with the clathrate solution.[35,36] Thus, it is demonstrated that copper is more stable in aqueous media in the presence of clathrates structures even in a high concentration of Cl^-. To ascertain that the stability of Cu is solely due to the fluid clathrate structure and not to the adsorption of $TtBA^+$ on the Cu surface, we carried out a cyclic voltammogram of a Cu wire in 0.6 m TtBACl aqueous solution and compare with the cyclic voltammogram obtained in the 1.8 m TtBACl. As shown in Figure S13, the obtained cyclic voltammograms show significant differences related to the Cu stability at potentials higher than 0.2 V where the current is still positive for the cyclic voltammogram in 0.6 m. Besides, cyclic voltammogram in 1.8 m KCl of the Cu wire after the experiment with the clathrate solution, in which the electrode surface was showing the presence of $TtBA^+$ by Raman is identical to the initially obtained in 1.8 m KCl (Figure 8a), ruling out the possibility that the adsorption of $TtBA^+$ on the metal surface is triggering the stability of the Cu electrode.

In summary, we have demonstrated the existence of a new type of supramolecular liquid, formed by (molten) semi-clathrate hydrate structures of composition $\approx TtBABr \cdot x\,H_2O$ $x = 38$–24, involving most of the water molecules in the solvent. Similar results were found in the corresponding Cl-salt, and in tetrabutyl-phosphonium bromide, suggesting a general behavior. In these fluids the structural fluctuations related to hydrophobic solvation of the alkyl chains dominate over the conventional H-bond (tetrahedral) structural fluctuations in bulk water. The change of the characteristic H-bond network of water results in a minimum compressibility and thermal diffusivity at room temperature, among other anomalies.

The results presented in this paper suggest an original approach for the design of a new class of supramolecular liquids, based on water solutions of small molecules containing a hydrophobic tail (probably with a symmetric disposition around a central atom). These supramolecular liquids could find important advanced technological applications as solvents and electrochemical media, sequestering agents for small non-polar molecules, etc.

Acknowledgements

We thank Dr. Francisco Ares of USC for kindly allowing us to use experimental facilities of his laboratory. This work was supported by the Ministry of Science of Spain (Projects No. PID2019-10415RB-I00, MAT2016-80762-R, RTI2018-101097-A-100, EIN2019-103246 and RyC-2016–20258), the Xunta de Galicia (ED431B 2018/16, 2018-AD006, 2018-PG070), the European Research Council (ERC) (StG-679124), the Consellería de Cultura, Educación e Ordenación Universitaria (ED431F 2016/008, and Centro singular de investigación de Galicia accreditation 2016–2019, ED431G/09), the Xunta de Galicia and the European Regional Development Fund (ERDF). C.L.-B. Acknowledges Xunta de Galicia and ESF for a PhD Grant (ED481A-2018/013).

Conflict of interest

The authors declare no conflict of interest.

Keywords: electrochemistry · hydrophobic solvation · liquid clathrate · supramolecular fluids · thermal diffusivity

[1] H. S. Frank, M. W. Evans, *J. Chem. Phys.* **1945**, *13*, 507–532.
[2] Y. L. A. Rezus, H. J. Bakker, *Phys. Rev. Lett.* **2007**, *99*, 148301.
[3] J. Grdadolnik, F. Merzel, F. Avbelj, *Proc. Natl. Acad. Sci. USA* **2017**, *114*, 322–327.
[4] Q. Sun, *Chem. Phys. Lett.* **2017**, *672*, 21–25.
[5] E. D. Sloan, *Nature* **2003**, *426*, 353–359.
[6] P. S. R. Prasad, B. Sai Kiran, *Sci. Rep.* **2018**, *8*, 8560.
[7] W. Shimada, T. Ebinuma, H. Oyama, Y. Kamata, S. Takeya, T. Uchida, J. Nagao, H. Narita, *Jpn. J. Appl. Phys.* **2004**, *43*, 362.
[8] D. L. Fowler, W. V. Loebenstein, D. B. Pall, C. A. Kraus, *J. Am. Chem. Soc.* **1940**, *62*, 1140–1142.
[9] M. Arjmandi, A. Chapoy, B. Tohidi, *J. Chem. Eng. Data* **2007**, *52*, 2153–2158.
[10] W. Shimada, M. Shiro, H. Kondo, S. Takeya, H. Oyama, T. Ebinuma, H. Narita, *Acta Crystallogr. Sect. C* **2005**, *61*, o65–o66.
[11] T. V. Rodionova, V. Y. Komarov, G. V. Villevald, T. D. Karpova, N. V. Kuratieva, A. Y. Manakov, *J. Phys. Chem. B* **2013**, *117*, 10677–10685.
[12] M. Tros, L. Zheng, J. Hunger, M. Bonn, D. Bonn, G. J. Smits, S. Woutersen, *Nat. Commun.* **2017**, *8*, 904.

[13] "The Clathrate Hydrates": G. A. Jeffrey, R. K. McMullan in *Progress in Inorganic Chemistry* (Ed.: F. A. Cotton), Wiley, New York, **1967**.
[14] G. Beurskens, G. A. Jeffrey, R. K. Mcmullan, *J. Chem. Phys.* **1963**, *39*, 3311.
[15] R. Mcmullan, G. A. Jeffrey, *J. Chem. Phys.* **1959**, *31*, 1231 – 1234.
[16] L. B. Skinner, C. J. Benmore, J. C. Neuefeind, J. B. Parise, *J. Chem. Phys.* **2014**, *141*, 214507.
[17] C. Huang, K. T. Wikfeldt, T. Tokushima, D. Nordlund, Y. Harada, U. Bergmann, M. Niebuhr, T. M. Weiss, Y. Horikawa, M. Leetmaa, M. P. Ljungberg, O. Takahashi, A. Lenz, L. Ojamäe, A. P. Lyubartsev, S. Shin, L. G. M. Pettersson, A. Nilsson, *Proc. Natl. Acad. Sci. USA* **2009**, *106*, 15214 – 15218.
[18] D. Schlesinger, K. T. Wikfeldt, L. B. Skinner, C. J. Benmore, A. Nilsson, L. G. M. M. Pettersson, *J. Chem. Phys.* **2016**, *145*, 084503.
[19] T. S. Banipal, S. K. Garg, J. C. Ahluwalia, *J. Chem. Thermodyn.* **1991**, *23*, 923 – 931.
[20] J. Chao, K. R. Hall, K. N. Marsh, R. C. Wilhoit, *J. Phys. Chem. Ref. Data* **1986**, *15*, 1369 – 1436.
[21] Y. U. Paulechka, A. G. Kabo, A. V. Blokhin, G. J. Kabo, M. P. Shevelyova, *J. Chem. Eng. Data* **2010**, *55*, 2719 – 2724.
[22] S. Woutersen, H. J. Bakker, *Nature* **1999**, *402*, 507 – 509.
[23] M. Christensen, A. B. Abrahamsen, N. B. Christensen, F. Juranyi, N. H. Andersen, K. Lefmann, J. Andreasson, C. R. H. Bahl, B. B. Iversen, *Nat. Mater.* **2008**, *7*, 811 – 815.
[24] O. Andersson, G. P. Johari, *J. Chem. Phys.* **2016**, *144*, 064504.
[25] J.-B. Brubach, A. Mermet, A. Filabozzi, A. Gerschel, P. Roy, *J. Chem. Phys.* **2005**, *122*, 184509.
[26] S. A. Rice, M. G. Sceats, *J. Phys. Chem.* **1981**, *85*, 1108 – 1119.
[27] T. A. Ford, M. Falk, *Can. J. Chem.* **1968**, *46*, 3579 – 3586.
[28] F. Li, J. L. Skinner, *J. Chem. Phys.* **2010**, *132*, 204505.
[29] see ref. [10]
[30] H. Tanaka, K. Nakanishi, K. Nishikawa, *Clathrate Compounds, Molecular Inclusion Phenomena, and Cyclodextrins*, Springer Netherlands, Dordrecht, **1984**, pp. 119 – 126.
[31] S. Gilman, *Electrochim. Acta* **1964**, *9*, 1025 – 1046.
[32] Y. Wang, B. Liu, X. Zhao, X. Zhang, Y. Miao, N. Yang, B. Yang, L. Zhang, W. Kuang, J. Li, E. Ma, Z. Shan, *Nat. Commun.* **2018**, *9*, 1 – 8.
[33] Y. Qiang, S. Fu, S. Zhang, S. Chen, X. Zou, *Corros. Sci.* **2018**, *140*, 111 – 121.
[34] A. R. Langley, M. Carta, R. Malpass-Evans, N. B. McKeown, J. H. P. Dawes, E. Murphy, F. Marken, *Electrochim. Acta* **2018**, *260*, 348 – 357.
[35] D. S. Zimbovskii, B. R. Churagulov, *Inorg. Mater.* **2018**, *54*, 660 – 666.
[36] L. C. Chen, C. C. Chen, K. C. Liang, S. H. Chang, Z. L. Tseng, S. C. Yeh, C. T. Chen, W. T. Wu, C. G. Wu, *Nanoscale Res. Lett.* **2016**, *11*, 402.

Manuscript received: November 26, 2020
Revised manuscript received: January 1, 2021
Accepted manuscript online: January 8, 2021
Version of record online: February 18, 2021

